

# The Relation Between Endohedral Chemical Shifts and Local Aromaticities in Fullerenes

Michael Bühl

**Abstract:** Chemical shifts of the centers of the pentagons and hexagons (termed nucleus-independent chemical shifts, NICS<sup>[15]</sup>) are reported for the fullerenes  $C_n$  ( $n = 32, 50, 60, 70, 76, 78, 84, 120, 180$ ) and some hexaanions thereof ( $n = 60, 70, 84$ ), as well as for  $C_{60}H_2$ , at the GIAO-SCF/DZP//BP86/3-21G level. Reflecting the ring current flows in the polycyclic carbon framework, the NICS

values can help to identify areas of higher local aromaticity or antiaromaticity (usually associated with hexagons and pentagons, respectively) in each fullerene. Even though corannulene- or

coronene-like patterns can be identified in some cases, the NICS values are not transferable from one species to another. According to a very simple, classical model, the endohedral chemical shifts at the center of the fullerenes can to a large extent be attributed to the ring currents in the individual five- and six-membered rings, as assessed by their NICS values.

**Keywords:** aromaticity • endohedral chemical shifts • fullerenes • NMR spectroscopy • ring currents

## Introduction

$^3\text{He}$  chemical shifts of endohedral helium fullerene compounds and derivatives thereof are so sensitive to the particular host molecule that the  $^3\text{He}$  labeling and NMR technique is a powerful analytical tool.<sup>[1, 2]</sup> Each isomer of a given, labeled fullerene (or any derivative) so far is characterized by a single peak in the  $^3\text{He}$  NMR spectrum with a distinctive  $^3\text{He}$  chemical shift.<sup>[2]</sup> The range of endohedral  $\delta(^3\text{He})$  values to date extends from  $\delta = -6.3$  ( $\text{He}@C_{60}$ ) to  $-28.8$  ( $\text{He}@C_{70}$ ) for neutral fullerenes,<sup>[2]</sup> and to  $-49$  for  $\text{He}@C_{60}^{6-}$ .<sup>[3]</sup> With pioneering Hückel-type London calculations, Haddon and coworkers qualitatively predicted the corresponding trends in the endohedral shieldings for  $C_{60}$ ,  $C_{70}$ , and  $C_{60}^{6-}$ .<sup>[4, 5]</sup> These trends are reproduced more quantitatively employing ab initio methods with small and medium-sized basis sets.<sup>[6-8]</sup>

Both experiment<sup>[9]</sup> and theory<sup>[8, 10, 11]</sup> find the endohedral chemical shifts of higher fullerenes in between those of  $C_{60}$  and  $C_{70}$ . Large endohedral shieldings have been predicted computationally for the smaller fullerenes (up to  $-46$  for  $\text{He}@C_{32}$ ) and nearly constant, intermediate values have been obtained for large, symmetric fullerenes ( $\delta \approx -17$  for  $\text{He}@C_{120}$  and  $\text{He}@C_{180}$ , at the GIAO-SCF/DZ//MNDO lev-

el),<sup>[11]</sup> but no clear-cut relation between  $\delta(\text{endo})$  and fullerene size has been found. Notable differences in  $\delta(\text{endo})$  values are apparent between fullerene isomers, for instance in the case of  $C_{84}$ , where one particular isomer,  $D_{2d}(4)$ , is characterized by an endohedral shift far outside the range covered by the other  $C_{84}$  isomers.<sup>[8]</sup>

In the endohedral helium compounds, the  $^3\text{He}$  nucleus acts as a probe for the ring-current effects due to the mobile  $\pi$  electrons of the fullerene host. Ring-current-induced chemical shifts (or other magnetic properties such as susceptibilities) can be used as indicators for aromaticity. From these criteria it has been concluded that  $C_{60}$  is of modest (or ambiguous) aromatic character, whereas those of  $C_{70}$  and especially  $C_{60}^{6-}$  are much larger.<sup>[12]</sup> Compared to the latter, the reduced aromaticity of the neutral fullerenes has been shown to arise from paratropic ring currents in the pentagons, which quench part of the diamagnetism due to the diatropic ring currents in the hexagons.<sup>[12, 13]</sup> The existence of such "segregated ring currents" has received support from  $^1\text{H}$  NMR spectroscopy of methanofullerenes.<sup>[14]</sup>

Is there a way to relate such ring currents in the fullerene framework to the endohedral chemical shifts at the very center of the cage? In the present paper, the local aromaticity and antiaromaticity of each ring in selected fullerenes is assessed by NICS (nucleus-independent chemical shift)<sup>[15]</sup> calculations. NICS values are theoretical chemical shifts of ring centers in cyclic or polycyclic compounds, which have recently been introduced as a simple and efficient probe for local aromaticity.<sup>[15]</sup> Aromatic and antiaromatic rings are associated with negative (i.e. shielded) and positive (i.e.

[\*] Dr. M. Bühl

Organisch-chemisches Institut  
Universität Zürich, Winterthurerstr. 190  
CH-8057 Zürich (Switzerland)  
Fax: (41) 1-635-6812  
E-mail: buehl@oci.unizh.ch

deshielded) NICS values, respectively, as illustrated by the data for the prototypical species benzene ( $\delta \approx -10$ ) and cyclobutadiene ( $\delta \approx +28$ )<sup>[15]</sup> Indeed, similar variations are computed for the fullerene NICS values. The NICS data are not transferable from one fullerene to the other, but can to a large extent be related to the endohedral chemical shifts in terms of a simple, classical ring-current model.

## Methods of Calculation

Geometries were fully optimized in the given symmetry at a gradient-corrected level of density functional theory (DFT), by means of Becke's 1988 exchange<sup>[16]</sup> and Perdew's 1986 correlation functional<sup>[17]</sup> standard 3-21G basis,<sup>[18]</sup> and a medium-sized grid (grid 3)<sup>[19]</sup> with the TURBOMOLE program.<sup>[20]</sup> In addition, higher-level geometries were employed for  $C_{60}$ <sup>[21]</sup> and  $C_{70}$ ,<sup>[8, 22]</sup> optimized at MP2/TZP and BP86/TZP levels, respectively. Magnetic shieldings were computed with the direct gauge-including atomic orbitals (GIAO)-SCF method as implemented<sup>[23]</sup> in TURBOMOLE, employing DZP basis, that is, a Huzinaga basis<sup>[24]</sup> contracted and augmented with polarization functions as follows: C (8s4p1d)/[4s2p1d],  $\alpha_d = 0.8$ ; H (4s1p)/[2s1p],  $\alpha_p = 0.8$ . Isotropic chemical shifts, reported as the magnetic shieldings with reversed sign, were evaluated for the centers of mass of each fullerene, denoted  $\delta(\text{endo})$ , and for the center of mass of each individual ring, denoted NICS.

## Results and Discussion

It appears that experimental endohedral  $^3\text{He}$  chemical shifts of endohedral helium fullerene compounds can be reproduced within ca. 2–3 ppm at the highest level employed so far, GIAO-SCF/DZP//BP86/3-21G, and that the theoretical values tend to be too shielded with respect to experiment.<sup>[8]</sup> The theoretical description of polyanions may be more difficult: for  $C_{60}^{6-}$ , a large endohedral shielding has been predicted,  $\delta = -58$  at the GIAO-SCF/DZ//SCF/6-31 + G level,<sup>[7]</sup> indicative of the aforementioned large degree of aromaticity. Very recently, a strongly shielded  $^3\text{He}$  resonance

has been recorded at  $\delta = -49$  and has been assigned to  $\text{He}@C_{60}^{6-}$ .<sup>[23]</sup> Refinement of the theoretical value at the higher GIAO-SCF/DZP//BP86/3-21G level affords  $\delta(\text{endo}) \approx -64$  (Table 1), not in very good agreement with experiment. According to a preliminary GIAO-SCF/DZ//MNDO calculation for  $C_{60}\text{Li}_6$ , counterion effects should be small, around 1 ppm.<sup>[25]</sup> Apart from possible medium effects, it may be that the lack of electron correlation in the present calculations is more severe for polyanions than for neutral fullerenes, which could account for much of the discrepancy with respect to the experimental  $\text{He}@C_{60}^{6-}$  results.

Despite these apparent shortcomings, hexaanions of  $C_{70}$  and  $D_{2d}(23)\text{-}C_{84}$  have been included in the present study. The computed  $\delta(\text{endo})$  values are approximately  $-11$  and  $-33$ , respectively, that is, considerably deshielded and shielded with respect to neutral  $C_{70}$  and  $C_{84}$ , respectively ( $\delta(\text{endo}) = -29$  and  $-12$ , respectively, at the same level), in accord with predictions from Hückel-type London calculations.<sup>[10]</sup>  $C_{84}$  may take up to six electrons, as endohedral compounds such as  $\text{Sc}_2@C_{84}$  are known (one particular isomer has recently been shown<sup>[26]</sup> to be derived from the  $D_{2d}(23)$  structure). According to ab initio and density functional calculations, only four electrons in  $\text{Sc}_2@C_{84}$  are transferred to the cage.<sup>[27]</sup> Therefore,  $C_{84}^{4-}$  has also been studied, and a somewhat reduced shielding (with respect to the hexaanion) is computed:  $\delta(\text{endo})$  is approximately  $-26$  (Table 1).

To what extent are these variations in  $\delta(\text{endo})$  reflected in the NICS values? Figure 1 summarizes the NICS values of selected neutral fullerenes  $C_n$  ( $n = 32, 50, 60, 70, 76, 78, 84, 120, 180$ ), the endohedral chemical shifts of which have been studied previously,<sup>[8, 11]</sup> and of some hexaanions  $C_n^{6-}$  ( $n = 60, 70, 84$ ). Consistent with the earlier studies of ring currents in  $C_{60}$ , local aromatic and antiaromatic character is found for hexagons and pentagons, respectively, with NICS values of  $\delta = -7$  and  $+7$ , respectively (comparable to the data reported in ref. [15], obtained with a somewhat different geometry and basis set); see Figure 1.

For the whole set of molecules in Figure 1, there are substantial variations of the NICS values within each fullerene and from one species to the other. Unfortunately, the NICS values do not seem to be transferable between the molecules, nor is there an apparent relation to the way the rings are connected. Some general trends, however, may be noted: For  $C_{60}$ ,  $C_{70}$ , and the higher fullerenes, the five-membered rings show local non- or antiaromatic character, with NICS values between ca.  $-2$  and  $+11$ . The six-membered rings usually display notable local aromaticity, but there are also examples of non- or slightly antiaromatic hexagons, and the NICS values cover the range between ca. 3 to  $-18$  (cf. the value for benzene,  $\delta = -10.8$  at the same level).

In many cases, the pattern of the NICS values around a pentagon bears some resemblance to that in corannulene (Figure 2). For  $C_{120}$  and  $C_{180}$ , which show the tendency towards formation of planar graphene-like substructures typical of the giant fullerenes,<sup>[28, 29]</sup> NICS patterns similar to that of coronene (Figure 2) can be identified, with the characteristic, nonaromatic central hexagon. For the smaller fullerenes  $C_{32}$  and  $C_{50}$ , more negative (i.e. more diamagnetic)

---

**Abstract in German:** *Chemische Verschiebungen für die Mittelpunkte von Fünf- und Sechsringen (nucleus-independent chemical shifts, NICSs<sup>[15]</sup>) wurden für die folgenden Spezies auf dem GIAO-SCF/DZP//BP86/3-21G-Niveau berechnet: Fullerene  $C_n$  ( $n = 32, 50, 60, 70, 76, 78, 84, 120, 180$ ), einige Hexaanionen derselben ( $n = 60, 70, 84$ ) sowie für  $C_{60}\text{H}_2$ . Die NICS-Werte spiegeln die Ringströme im polyzyklischen Kohlenstoffgerüst wieder und können dazu beitragen, Gebiete erhöhter lokaler Aromatizität bzw. Antiaromatizität zu identifizieren (die für gewöhnlich mit Sechs- bzw. Fünfringen verknüpft sind). Zwar können in manchen Fällen Corannulen- oder Coronen-ähnliche Muster ausgemacht werden, doch sind die NICS-Werte nicht von einer Spezies auf die andere übertragbar. Mit einem sehr einfachen klassischen Modell können die endohedralen chemischen Verschiebungen des Fullerenzentrums zum großen Teil auf die aus den NICS-Werten abgeschätzten Ringströme der einzelnen Fünf- und Sechsringe zurückgeführt werden.*

---

Table 1. NICS values (GIAO-SCF/DZP//BP86/3-21G level), distances  $z$  from the center (Å), and individual contributions  $\delta(\text{RC})$  [from Eq. (1)].<sup>[a]</sup>

Molecule [ $\delta(\text{endo})$ ]	NICS	(Mult.) <sup>[b]</sup>	$z$	$\delta(\text{RC})$ [ $\Sigma \delta(\text{RC})$ ] <sup>[c]</sup>	Molecule [ $\delta(\text{endo})$ ]	NICS	(Mult.) <sup>[b]</sup>	$z$	$\delta(\text{RC})$ [ $\Sigma \delta(\text{RC})$ ] <sup>[c]</sup>
C <sub>32</sub> [−52.7]	−12.51 <sup>[d]</sup>	(6)	2.430	−0.82	C <sub>84</sub> (4) [−25.0]	0.73 <sup>[d]</sup>	(4)	4.431	0.01
	−18.35 <sup>[d]</sup>	(6)	2.229	−1.49		3.46 <sup>[d]</sup>	(4)	4.238	0.05
	−26.36	(6)	2.137	−3.71		0.96 <sup>[d]</sup>	(4)	3.816	0.02
C <sub>50</sub> [−36.6]	−12.21 <sup>[d]</sup>	(2)	2.791	−0.56	−8.92	(4)	4.483	−0.19	
	−6.71 <sup>[d]</sup>	(10)	3.107	−0.23	−13.43	(8)	3.820	−0.45	
	−17.93	(10)	2.851	−1.28	−11.70	(8)	4.105	−0.32	
	−11.12	(5)	3.032	−0.68	−6.90	(8)	3.675	−0.26	
				−19.7	−15.40	(4)	3.909	−0.49	
C <sub>60</sub> [−11.2]	7.00 <sup>[d]</sup>	(12)	3.352	0.20	C <sub>120</sub> [−19.6]	7.52 <sup>[d]</sup>	(12)	5.192	0.06
	−6.61	(20)	3.276	−0.33		−5.47	(4)	5.401	−0.07
C <sub>60</sub> <sup>[e]</sup> //MP2/TZP [−8.5]	8.89 <sup>[d]</sup>	(12)	3.327	0.26	−10.39	(12)	5.042	−0.16	
	−5.31	(20)	3.248	−0.27	−11.31	(24)	4.622	−0.23	
C <sub>70</sub> [−28.5]	1.64 <sup>[d]</sup>	(2)	3.993	0.03	−0.21	(4)	4.351	0.00	
	−2.29 <sup>[d]</sup>	(10)	3.655	−0.05	0.08	(6)	4.595	0.00	
	−12.73	(10)	3.792	−0.44				−6.9	
	−10.50	(10)	3.445	−0.46	C <sub>180</sub> [−18.5]	10.88 <sup>[d]</sup>	(12)	6.235	0.05
	−17.73	(5)	3.370	−0.83		−9.52	(60)	6.010	−0.09
			−13.6	3.38	(20)	5.913	0.03		
C <sub>70</sub> <sup>[f]</sup> //BP86/TZP [−29.3]	2.01 <sup>[d]</sup>	(2)	3.973	0.04	C <sub>60</sub> <sup>6−</sup> [−64.4]	−28.80 <sup>[d]</sup>	(12)	3.384	−0.79
	−2.21 <sup>[d]</sup>	(10)	3.634	−0.05	−29.40	(20)	3.301	−1.45	
	−12.96	(10)	3.769	−0.45				−38.5	
	−10.73	(10)	3.428	−0.48	C <sub>70</sub> <sup>6−</sup> [−10.6]	−14.94 <sup>[d]</sup>	(2)	4.018	−0.25
	−17.85	(5)	3.354	−0.84	−16.65 <sup>[d]</sup>	(10)	3.688	−0.36	
			−14.0	−5.54	(10)	3.803	−0.19		
C <sub>76</sub> [−20.4]	1.46 <sup>[d]</sup>	(4)	3.997	0.03	−3.92	(10)	3.474	−0.17	
	5.69 <sup>[d]</sup>	(4)	4.097	0.09	−2.22	(5)	3.408	−0.10	
	3.21 <sup>[d]</sup>	(4)	3.705	0.07				−8.2	
	−9.07	(4)	4.145	−0.24	C <sub>84</sub> (23) <sup>6−</sup> [−32.7]	−23.81 <sup>[d]</sup>	(4)	4.089	−0.39
	−7.99	(4)	3.719	−0.29		−20.64 <sup>[d]</sup>	(8)	4.132	−0.33
	−13.34	(4)	3.569	−0.54		−14.77	(4)	4.048	−0.42
	−8.00	(4)	3.984	−0.24		−14.26	(8)	3.987	−0.43
	−6.55	(4)	3.756	−0.23		−15.36	(4)	3.864	−0.50
	−15.15	(4)	3.608	−0.59		−14.31	(4)	4.051	−0.41
	−4.38	(4)	3.300	−0.22		−14.42	(8)	3.979	−0.43
				−8.6		−12.10	(4)	3.985	−0.36
			−7.1					−17.8	
			−7.1	C <sub>84</sub> (23) <sup>4+</sup> [−26.3]		−20.73 <sup>[d]</sup>	(4)	4.068	−0.34
			−7.1		−0.71 <sup>[d]</sup>	(8)	4.123	−0.01	
			−7.1		−8.51	(4)	4.020	−0.25	
			−7.1		−12.16	(8)	3.976	−0.37	
			−7.1		−5.82	(4)	3.858	−0.19	
			−7.1		−12.90	(4)	3.975	−0.39	
			−7.1		−12.81	(8)	4.040	−0.37	
			−7.1		−14.11	(4)	3.976	−0.42	
			−7.1					−12.4	
			−7.1					−12.4	
C <sub>84</sub> (23) [−11.9]	9.50 <sup>[d]</sup>	(4)	4.040	0.16					
	7.41 <sup>[d]</sup>	(8)	4.107	0.12					
	−11.88	(8)	3.963	−0.36					
	2.10	(4)	3.847	0.07					
	−4.10	(8)	3.964	−0.12					
	−0.45	(4)	4.005	−0.01					
	0.06	(4)	4.033	0.00					
	−10.26	(4)	3.977	−0.31					
			−3.3						

[a]  $\delta(\text{RC})$  is calculated as the corresponding NICS value multiplied by the expression given in Equation (1), see also ref. [31]; two loop radii  $a$  have been used for all five- and six-membered rings, chosen so that the enclosed areas are the same as those of a pentagon and a hexagon with an (average) C–C bond length of 1.46 and 1.43 Å, respectively. [b] Number of symmetry-equivalent rings. [c] Sum of  $\delta(\text{RC})$  values of all rings. [d] Five-membered ring. [e] MP2/6-31G\* geometry employed. [f] BP86/TZP geometry employed.

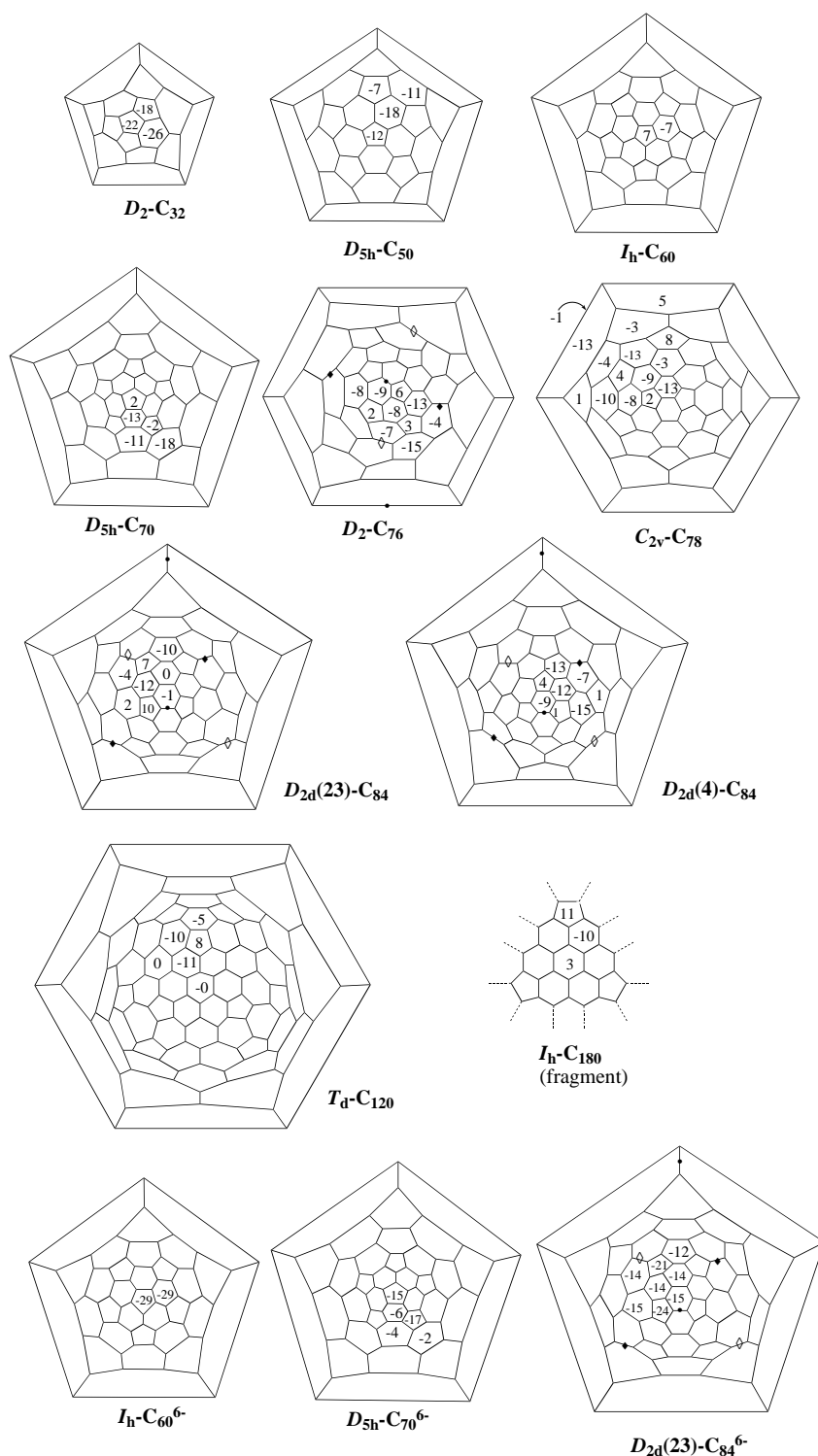


Figure 1. Schlegel plots of fullerenes and fullerene hexaanions, including the GIAO-SCF/DZP//BP86/3-21G computed NICS values of the individual rings (values not shown are determined by symmetry). For the  $D_2$  and  $D_{2d}$  symmetric species, the locations of the twofold axes are indicated at the appropriate C–C bonds. For  $C_{180}$ , only a section along one of the threefold axes is shown.

NICS values are computed, to  $-26$  (Figure 1). In the hexaanions, all pentagons have substantial local aromatic character (NICS values from  $\delta = -15$  to  $-29$ ), while the local aromaticity of the six-membered rings is small for  $C_{70}^{6-}$  (NICS between  $-2$  and  $-6$ ), large for  $D_{2d}(23)-C_{84}^{6-}$  (NICS between

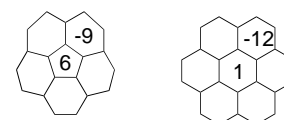


Figure 2. NICS values for corannulene (left) and coronene (right), GIAO-SCF/DZP//BP86/3-21G level.

$-12$  and  $-15$ ), and very large for  $C_{60}^{6-}$  ( $-29$ ).

How can the NICS values from Figure 1 be related to the endohedral chemical shifts? As a very simple model, one may assume that the chemical shift in the center of each ring originates solely from current loops around that ring (this is certainly a very crude approximation, since anisotropy effects of the  $\sigma$  bonds nearby should also contribute to the NICS values, if only by a small and presumably fairly constant amount). From classical electrodynamics, the magnetic field and, thus, the chemical shift, can be calculated at any point in space around a circular current loop. On a line through the center and perpendicular to the plane of the loop, the magnetic field  $B_{\text{ind}}$  should be proportional to the expression in Equation 1, where  $a$  is the radius of the

$$B_{\text{ind}} \propto a^2/(a^2 + z^2)^{3/2} \quad (1)$$

loop and  $z$  the distance from the center.<sup>[30]</sup> From the NICS value of a given ring and its distance from the center, one can therefore estimate the ring current contribution of this ring to  $\delta(\text{endo})$ , denoted  $\delta(\text{RC})$ .<sup>[31]</sup>

The relevant data are collected in Table 1, and the sum of all  $\delta(\text{RC})$  values for each fullerene is plotted against  $\delta(\text{endo})$  in Figure 3. There is in fact a fairly good correlation between these quantities. The slope of 0.7 suggests that a substantial part of the endohedral chemical shifts can be attributed to ring currents localized in the individual pentagons and hexagons. The remaining fraction of  $\delta(\text{endo})$  probably arises from ring currents enclosing larger areas, in particular around the perimeters of the fullerene cages, which are only partially

included in the NICS values. According to London calculations,<sup>[5]</sup> no such larger ring currents are present in  $C_{70}^{6-}$ , which may thus account for the noticeable deviation from the overall fit of this particular data point (open square at  $\delta \approx -10$ , Figure 3).

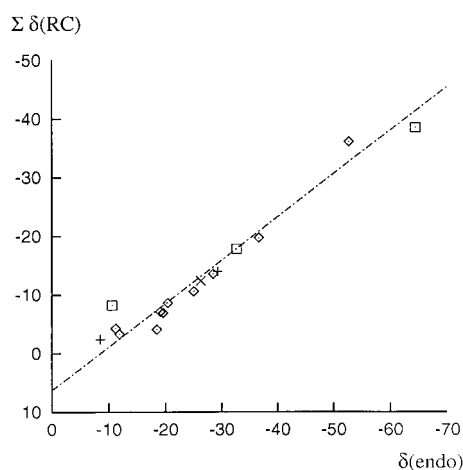


Figure 3. Plot of the sum of all NICS contributions to  $\delta(\text{endo})$ ,  $\Sigma\delta(\text{RC})$ , vs.  $\delta(\text{endo})$ . The straight line is a fit to all data points (slope = 0.7);  $\diamond$  neutral fullerenes,  $\square$  hexaanions,  $\times$   $\text{C}_{84}^+$  (BP86/3-21G geometries),  $+$   $\text{C}_{60}$  and  $\text{C}_{70}$  from MP2/TZP and BP86/TZP geometries, respectively.

Inspection of the data in Table 1 reveals that the absolute contributions  $\delta(\text{RC})$  of the five-membered rings are always smaller than those of the six-membered rings, because of the smaller radius  $a$  of the former. Variations in  $\delta(\text{endo})$  from one fullerene to another (or to another isomer) thus appear to be less sensitive to changes in the local paratropic currents in the pentagons, but seem to be more strongly affected by the diatropicity of the hexagons. In the case of the two  $\text{C}_{84}$  isomers, for instance, the average NICS values of the pentagons differ strongly ( $\delta \approx 8$  and  $2$  for isomer 23 and 4, respectively), but their total contributions to  $\delta(\text{endo})$  are small ( $\delta(\text{RC}) = 1.6$  and  $0.3$ , respectively). Almost all of the calculated change in  $\Sigma\delta(\text{RC})$  between both isomers (and, thus, more than half of the computed change in  $\delta(\text{endo})$ ) is attributable to the variation of the diatropicity of the hexagons, as assessed by their NICS values.

The  $x$ -intercept in Figure 3 ( $\delta = -8.5$  at  $\Sigma\delta(\text{RC}) = 0$ ) suggests that part of the observed endohedral shielding may not be due to ring-current effects in the  $\pi$ -system, but may rather arise from anisotropy effects of the  $\sigma$  framework. The same conclusion can be drawn from calculations for the fully hydrogenated species  $\text{He}@C_{60}\text{H}_{60}$  and  $\text{He}@C_{70}\text{H}_{70}$ , for both of which  $^3\text{He}$  chemical shifts of ca.  $-5$  are obtained at the GIAO-SCF/DZ//SCF/3-21G level.<sup>[7]</sup>

How are the current flows affected when exohedral adducts are formed? Trends in the endohedral  $^3\text{He}$  chemical shifts upon exohedral derivatization of the fullerene cages have been studied experimentally in some detail.<sup>[2, 32]</sup> Some effects on  $\delta(^3\text{He})$  can be remarkably large: for instance, the removal of one double bond from  $\text{C}_{60}$  by monoadduct formation is paralleled by an increased endohedral shielding of ca.  $2$ – $3$  ppm. That each derivative so far is characterized by a single, well-separated  $\delta(^3\text{He})$  resonance is one of the reasons for the great analytical potential of the  $^3\text{He}$  labeling and NMR technique.

$\text{C}_{60}\text{H}_2$  is the prototypical example for a  $\text{C}_{60}$  adduct. Addition occurs in a [6,6] fashion,<sup>[33]</sup> that is, at an edge shared by two hexagons. The effect on the endohedral chemical shift is remarkable: In going from  $\text{C}_{60}$  to  $\text{C}_{60}\text{H}_2$ ,  $\delta(\text{endo})$  is computed

to become more shielded by  $\Delta\delta = -2.0$  at the GIAO-SCF/DZP//BP86/3-21G level, in reasonable accord with the increase in the corresponding  $\delta(^3\text{He})$  shielding of  $\Delta\delta = -3.3$  found experimentally.<sup>[34]</sup> It is tempting to speculate that the effective removal of a double bond connecting two pentagons would destroy the paramagnetic current flows in the latter and thus account for the increased shielding at the center. The NICS values in Figure 4 confirm this general picture and

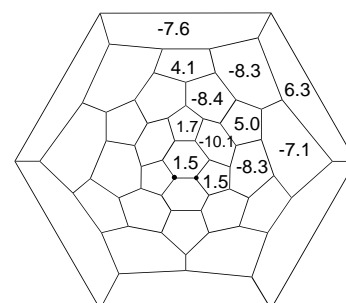


Figure 4. NICS values for  $\text{C}_{2v}\text{-C}_{60}\text{H}_2$ , computed at the GIAO-SCF/DZP//BP86/3-21G level. The hydrogenated carbon atoms are denoted by filled circles.

reveal some interesting additional details. Firstly, the dia- and paratropic ring currents are not only essentially quenched in the two pentagons and hexagons that bear the saturated carbon atoms, but also in the two next-nearest five-membered rings. Secondly, the local diatropicity of almost all of the other six-membered rings is somewhat increased (NICS values between ca.  $-7$  and  $-10$ ) with respect to that in  $\text{C}_{60}$  ( $-7.0$  at the same level), whereas the paratropicity in the remaining pentagons (NICS values between  $4$  and  $6$ ) is slightly reduced (corresponding NICS value in  $\text{C}_{60}$ :  $6.6$ , cf. Table 1).

If one sums up all the NICS contributions  $\delta(\text{RC})$  to  $\delta(\text{endo})$  as outlined above, one arrives at a value of  $-6.3$ , that is, exactly  $2$  ppm more shielded than the corresponding number for  $\text{C}_{60}$  (Table 1). Interestingly, the total contributions  $\delta(\text{RC})$  of the two hexagons and four pentagons closest to the CH sites are only  $-0.3$  (compared with ca.  $-0.1$  for the same number of rings in  $\text{C}_{60}$ ). It thus appears that the notable shielding of endohedral  $^3\text{He}$  upon adduct formation is largely due to local changes of ring currents, but these changes are associated with virtually all of the rings rather than concentrated on those closest to the site of adduct formation. It will be interesting to see if NICS calculations can aid in the interpretations of trends in  $\delta(^3\text{He})$  upon multiple adduct formation.<sup>[32, 35]</sup>

## Conclusion

In summary, even though the NICS values are not transferable from one species to another, they are useful as an interpretative tool by identifying regions of high local aromaticity and antiaromaticity in fullerenes and derivatives thereof. The notion that the endohedral chemical shifts originate from ring currents in the fullerene cages is borne out by the NICS calculations: according to a simple, classical

model, a large part of the endohedral chemical shifts of the fullerenes is attributable to local dia- and paratropic ring currents in the individual hexagons and pentagons. Thus, effects on the  $\delta(\text{endo})$  values can be assessed in terms of contributions from each ring.

**Acknowledgments:** The author wishes to thank W. Thiel for continuous support and P. von R. Schleyer, R. C. Haddon, and M. Saunders for discussions. The calculations were carried out on IBM RS6000 workstations at the University (Organisch-chemisches Institut) and at the ETH Zürich (C4 cluster).

Received: August 17, 1997 [F791]

- [1] M. Saunders, H. A. Jiménez-Vázquez, R. J. Cross, S. Mroczkowski, D. I. Freedberg, F. A. L. Anet, *Nature* **1994**, *367*, 256–258.
- [2] Review: M. Saunders, R. J. Cross, H. A. Jiménez-Vázquez, R. Shimshi, A. Khong, *Science* **1996**, *271*, 1693–1697.
- [3] M. Saunders, M. Rabinovitz, private communication (results reported by M.R. in a talk given in Zürich, January **1997**).
- [4] A. Pasquerello, M. Schlüter, R. C. Haddon, *Science* **1992**, *257*, 1660–1661.
- [5] A. Pasquerello, M. Schlüter, R. C. Haddon, *Phys. Rev. A* **1993**, *47*, 1783–1789.
- [6] J. Cioslowski, *J. Am. Chem. Soc.* **1994**, *116*, 3619–3620.
- [7] M. Bühl, W. Thiel, H. Jiao, P. von R. Schleyer, M. Saunders, F. A. L. Anet, *J. Am. Chem. Soc.* **1994**, *116*, 6005–6006.
- [8] M. Bühl, C. v. Wüllen, *Chem. Phys. Lett.* **1995**, *247*, 63–68.
- [9] M. Saunders, H. A. Jiménez-Vázquez, R. J. Cross, W. E. Billups, C. Gesenberg, A. Gonzales, W. Luo, R. C. Haddon, F. Diederich, A. Herrmann, *J. Am. Chem. Soc.* **1995**, *117*, 9305–9308.
- [10] R. C. Haddon, A. Pasquerello, *Phys. Rev. B* **1994**, *50*, 16459–16463.
- [11] M. Bühl, W. Thiel, *Chem. Phys. Lett.* **1995**, *233*, 585–589.
- [12] R. C. Haddon, *Science* **1993**, *261*, 1545–1550.
- [13] R. Zanasi, P. W. Fowler, *Chem. Phys. Lett.* **1995**, *238*, 270–280.
- [14] M. Prato, V. Lucchini, M. Maggini, E. Stimpfl, G. Scorrano, M. Eiermann, T. Suzuki, F. Wudl, *J. Am. Chem. Soc.* **1993**, *115*, 8479–8480.
- [15] P. von R. Schleyer, C. Maerker, A. Dransfeld, H. Jiao, N. J. R. van E. Hommes, *J. Am. Chem. Soc.* **1996**, *118*, 6317–6318.
- [16] A. D. Becke, *Phys. Rev. A* **1988**, *38*, 3098–3100.
- [17] J. P. Perdew, *Phys. Rev. B* **1986**, *33*, 8822–8824; *ibid.* **1986**, *34*, 7046.
- [18] W. Hehre, L. Radom, P. von R. Schleyer, J. A. Pople, *Ab Initio Molecular Orbital Theory*, Wiley, New York, **1986**.
- [19] O. Treutler, R. Ahlrichs, *J. Chem. Phys.* **1995**, *102*, 346–354.
- [20] R. Ahlrichs, M. Bär, M. Häser, H. Horn, M. Kölmel, *Chem. Phys. Lett.* **1989**, *154*, 165–169.
- [21] M. Häser, J. Almlöf, G. E. Scuseria, *Chem. Phys. Lett.* **1991**, *181*, 497–500.
- [22] K. Hedberg, L. Hedberg, M. Bühl, D. S. Bethune, C. A. Brown, R. D. Johnson, *J. Am. Chem. Soc.* **1997**, *119*, 5314–5320.
- [23] M. Häser, R. Ahlrichs, H. P. Baron, P. Weiss, H. Horn, *Theor. Chim. Acta* **1992**, *83*, 455–470.
- [24] S. Huzinaga, *Approximate Atomic Wave Functions*, University of Alberta, Edmonton, **1971**.
- [25] M. Bühl, unpublished calculations.
- [26] E. Yamamoto, M. Tansho, T. Tomiyama, H. Shinohara, *J. Am. Chem. Soc.* **1996**, *118*, 2293–2294.
- [27] K. Kobayashi, S. Nagase, T. Akasaka, *Chem. Phys. Lett.* **1996**, *261*, 502–506.
- [28] G. E. Scuseria, *Chem. Phys. Lett.* **1995**, *243*, 193–198.
- [29] D. Bakowies, M. Bühl, W. Thiel, *J. Am. Chem. Soc.* **1995**, *117*, 10113–10118; *Chem. Phys. Lett.* **1995**, *247*, 491–493.
- [30] W. R. Smythe, *Static and Dynamic Electricity*, 3rd ed, McGraw-Hill, New York, **1968**.
- [31] NICS values are isotropic, that is, scalar values. If the assumption were exactly fulfilled that they arise solely from circular current loops in the plane, then the NICS value of each ring could be viewed as vector with an out-of-plane component three times this NICS value and the in-plane components equal to zero. Thus, the component of  $\delta(\text{RC})$  at the fullerene center pointing toward a given ring would be three times the respective value given in Table 1. Since the other two components of  $\delta(\text{RC})$  would be zero, the tabulated values correspond to the isotropic average. The vector sums of all rings do not cancel in centrosymmetric fullerenes because the direction of each vector is the same with respect to the external field (e.g., always opposite to the latter for diatropic ring currents).
- [32] M. Rüttimann, R. F. Haldimann, L. Isaacs, F. Diederich, A. Khong, H. Jiménez-Vázquez, R. J. Cross, M. Saunders, *Chem. Eur. J.* **1997**, *3*, 1071–1076.
- [33] C. C. Henderson, P. A. Cahill, *Science* **1993**, *259*, 1885–1887.
- [34] S. R. Wilson, J. Cao, Q. Lu, Y. Wu, N. Kaprinidas, G. Lem, M. Saunders, H. A. Jiménez-Vázquez, D. I. Schuster, in *Science and Technology of Fullerene Materials* (Ed.: P. Bernier), Pittsburgh (PA), **1995**, p. 357–362.
- [35] W. E. Billups, W. Luo, A. Gonzalez, D. Arguello, L. B. Alemany, T. Mariott, M. Saunders, H. A. Jiménez-Vázquez, A. Khong, *Tetrahedron Lett.* **1997**, *38*, 171–174.